[mAbs 1:4, 364-369; July/August 2009]; ©2009 Landes Bioscience

Report

Identification of circulating neuropilin-1 and dose-dependent elevation following anti-neuropilin-1 antibody administration

Yanmei Lu,[1,*] Hong Xiang,[2] Peter Liu,[3] Raymond R. Tong,[3] Ryan J. Watts,[4] Alexander W. Koch,[3] Wendy N. Sandoval,[3] Lisa A. Damico,[2] Wai Lee Wong[1] and Y. Gloria Meng[1]

Departments of [1]Assay and Automation Technology; [2]Early development Pharmacokinetics and Pharmacodynamics; [3]Protein Chemistry and [4]Neurodegeneration; Genentech Inc.; South San Francisco, CA USA

Abbreviations: NRP1, neuropilin-1; VEGF, vascular endothelial growth factor; ECD, extracellular domain; sNRP1, soluble neuropilin-1; ELISA, enzyme-linked immunosorbent assay; PBS, phosphate-buffered saline; SDS-PAGE, sodium dodecyl sulfate-polyacrylamide gel electrophoresis; IP, immunoprecipitate; IB, immunoblot

Key words: angiogenesis, soluble neuropilin-1, circulating neuropilin-1, anti-neuropilin-1, ELISA, serum

Neuropilin-1 (NRP1) acts as a co-receptor for class 3 semaphorins and vascular endothelial growth factor and is an attractive angiogenesis target for cancer therapy. In addition to the transmembrane form, naturally occurring soluble NRP1 proteins containing part of the extracellular domain have been identified in tissues and a cell line. We developed ELISAs to study the existence of circulating NRP1 and to quantify it in serum. As measured by ELISAs, circulating NRP1 levels in mice, rats, monkeys and humans were 427 ± 77, 20 ± 3, 288 ± 86 and 322 ± 82 ng/ml (mean ± standard deviation; n ≥ 10), respectively. Anti-NRP1^B, a human monoclonal antibody, has been selected from a synthetic phage library. A 4-fold increase in circulating NRP1 was observed in mice receiving a single dose of 10 mg/kg anti-NRP1^B antibody. In rats and monkeys receiving single injections of anti-NRP1^B at different dose levels, higher doses of antibody resulted in greater and more prolonged increases in circulating NRP1. Maximum increases were 56- and 7-fold for rats and monkeys receiving 50 mg/kg anti-NRP1^B, respectively. In addition to the soluble NRP1 isoforms, for the first time, a ~120 kDa circulating NRP1 protein containing the complete extracellular domain was detected in serum by western blot and mass spectrometry analysis. This protein increased more than the putative soluble NRP1 bands in anti-NRP1^B treated mouse, rat and monkey sera compared with untreated controls, suggesting that anti-NRP1^B induced membrane NRP1 shedding.

*Correspondence to: Yanmei Lu; Department of Assay and Automation Technology; Genentech, Inc.; 1 DNA Way; South San Francisco, CA 94080 USA; Tel.: 650.225.8793; Fax: 650.225.1770; Email: yanmei@gene.com

Submitted: 02/27/09; Accepted: 04/29/09

Previously published online as a *mAbs* E-publication:
http://www.landesbioscience.com/journals/mabs/article/8885

Introduction

Neuropilin-1 (NRP1), a 130–140 kDa transmembrane glycoprotein, was initially identified as a receptor for class 3 semaphorins, which are negative mediators of neuronal guidance.[1,2] NRP1 also functions as a co-receptor for vascular endothelial growth factor (VEGF) and enhances $VEGF_{165}$ activities, such as endothelial cell migration.[3] NRP1 transgenic mice have excessive capillaries and blood vessels,[4] whereas NRP1 knockout mice display severe defects in vascular and axon development.[5,6]

NRP1 has a large extracellular domain (ECD), a single transmembrane domain and a short cytoplasmic tail that does not contain a kinase domain, but may mediate signaling through binding to a PDZ domain containing protein.[7-9] The extracellular portion of NRP1 contains several subdomains: a1a2 (two CUB motifs), a semaphorin 3 ligand-binding domain; b1b2 (two coagulation factor V/VIII domains), a VEGF binding domain; and c (MAM) domain implicated in NRP1 dimerization.[1,10-12] Cross-reactive antibodies that bound to both human and mouse NRP1 were selected from a human antibody phage library.[13] Anti-NRP1^B antibody binds to the b1b2 domain of NRP1 and blocks VEGF interaction with NRP1. This antibody reduces $VEGF_{165}$-dependent endothelial cell migration and vessel sprouting in vitro, neovascularization and vascular remodeling in vivo. It also inhibits tumor growth in a variety of mouse xenograft models, shows an additive effect with anti-VEGF treatment, and therefore, may be a useful agent for enhancing anti-angiogenesis therapy.[14]

In addition to the full-length transmembrane form, four naturally occurring human soluble NRP1 (sNRP1) isoforms were cloned.[15-17] These sNRP1 proteins contain only the a1a2 and b1b2 domains and lack the MAM, transmembrane and intracellular domains. They are generated by alternative splicing or by reading through into the intron, resulting in premature truncation. Cackowski et al. made recombinant proteins of three out

of the four sNRP1 isoforms that showed molecular weights of 90, 67 and 60 kDa,[15] but only the 90 kDa endogenous sNRP1 was reported in culture media of human PC3 cells.[16] The 90 and 67 kDa sNRP1 proteins contain intact a1a2 and b1b2 domains, whereas the 60 kDa sNRP1 is missing 48 amino acids at the C terminus of the b2 domain. Despite this, all three recombinant sNRP1 proteins bind to $VEGF_{165}$ or semaphorin 3A with affinities similar to that of cell surface NRP1 and function as antagonists for $VEGF_{165}$ in promoting cell migration.[15] In mouse, a 60 kDa sNRP1 protein was detected in liver.[18] sNRP1 from rat or monkey has not been reported.

Here we report the identification of circulating NRP1 in mouse, rat, monkey and human sera, and its dose-dependent increase following anti-$NRP1^B$ administration. Using western blot analysis, we detected not only the putative sNRP1 bands, but also a high molecular weight band corresponding to the complete NRP1 ECD in mouse, rat, monkey and human sera. Mass spectrometry analysis confirmed that this band in human serum contained the MAM domain, indicating that the circulating NRP1 measured by enzyme-linked immunosorbent assay (ELISA) includes both sNRP1 and NRP1 ECD.

Results

Circulating NRP1 levels in normal mouse, rat, cynomolgus monkey and human sera. Concentrations of circulating NRP1 in rodent and primate sera were measured by ELISAs using goat anti-rat NRP1 ECD and rabbit anti-human sNRP1 polyclonal antibodies, respectively. The assays were specific and did not cross-react with a homologous molecule, soluble neuropilin-2, at 300 ng/ml and 2,000 ng/ml in the rodent and primate sNRP1 ELISAs, respectively. Both assays also showed good accuracy and reproducibility. The inter- or intra-assay coefficients of variation calculated from ten independent experiments are ≤9.2% for rodent and ≤10.3% for primate assays.

The mean concentrations and ranges of circulating NRP1 in athymic nude mouse, Sprague-Dawley rat, cynomolgus monkey and healthy human sera are presented in Table 1. Serum from athymic nude mice was used because this strain was used in later anti-$NRP1^B$ animal studies to minimize anti-drug antibody responses. Pooled sera from CD-1 mouse showed comparable level of circulating NRP1 as athymic nude mice (data not shown). It is noteworthy that the mean level of circulating NRP1 detected in rats was approximately 10-fold lower than those measured in the other three species.

Anti-$NRP1^B$ treatment induced dose dependent increases in serum circulating NRP1 level. We next examined the effect of anti-$NRP1^B$ antibody treatment on circulating NRP1 levels using ELISAs. The rodent and primate assays measure total circulating NRP1, including free and anti-$NRP1^B$ bound forms, in the presence of up to 0.8 and 1.0 mg/ml anti-$NRP1^B$, respectively. In mice receiving a single intravenous dose of 10 mg/kg anti-$NRP1^B$ human monoclonal antibody, circulating NRP1 concentrations increased shortly after injection and reached a peak of 1.7 μg/ml on day 2 (4-fold greater than untreated), then returned to baseline levels (Fig. 1A) as the anti-$NRP1^B$ drug concentration decreased (data not shown). In contrast, in mice dosed with 10 mg/kg anti-$NRP1^A$, which is a human monoclonal antibody against the a1a2 domain of NRP1,[13,14] no significant increase in circulating NRP1 level was observed (data not shown). Next, we evaluated whether peak circulating NRP1 concentrations corresponded to the anti-$NRP1^B$ dose levels in rats. Compared to prebleeds, circulating NRP1 levels reached maximum fold increases of 16 ± 5 (day 1), 42 ± 20 (day 2) and 56 ± 14 (day 5) after single intravenous injections of 2, 10 and 50 mg/kg anti-$NRP1^B$, respectively (Fig. 1B). This anti-$NRP1^B$ dose-dependent increase in circulating NRP1 was also observed in cynomolgus monkeys (Fig. 1C). The maximum fold increases of 1.4 ± 0.2 (day 2), 2.6 ± 0.5 (day 3), 5.1 ± 1.5 (day 13) and 6.8 ± 1.2 (day 16) were obtained for single dose groups of 0.5, 3, 15 and 50 mg/kg, respectively, while circulating NRP1 remained at baseline levels in the phosphate-buffered saline (PBS) vehicle treated group. These data indicate that the higher the antibody dose level, the greater and more prolonged the increase of circulating NRP1.

Table 1 **Circulating NRP1 levels in mouse, rat, monkey and human sera**

Species	n	Circulating NRP1 (ng/ml)	
		Mean ± S.D.	Range
Mouse	10	427 ± 77	277–541
Rat	29	20 ± 3	11–28
Monkey	28	288 ± 86	162–469
Human	66	322 ± 82	146–618

In a multiple-dose rat safety study, five intravenous doses of anti-$NRP1^B$ were given at 10 mg/kg with a 3-day dose interval. Circulating NRP1 reached 0.9 μg/ml on day 3 and remained at this level through day 15 (Fig. 1D) when the drug concentration was maintained at ≥26 μg/ml (data not shown). Circulating NRP1 declined after day 15 as the anti-$NRP1^B$ concentration started to drop. No increase in circulating NRP1 level was observed in the PBS vehicle treated group. These data clearly show that the increase in circulating NRP1 is related to the anti-$NRP1^B$ drug level.

Western blot and mass spectrometry analysis of circulating NRP1 in serum. Circulating NRP1 proteins in sera from anti-$NRP1^B$ treated or untreated mice and rats were analyzed by western blotting using anti-rat NRP1 ECD antibody. In untreated mouse serum (Fig. 2A, lane 1), a novel ~120 kDa band was detected in addition to a ~64 kDa doublet band (in lighter exposure) which may correspond to the reported 60 kDa sNRP1 in mouse liver.[18] In untreated rat serum (lane 3), ~75 and ~120 kDa bands were visible. In agreement with the ELISA results, the band intensities in serum from untreated rat were much weaker than those of mouse. After administration of 10 mg/kg anti-$NRP1^B$, significant increases in band intensities were observed in mouse (day 2 serum) (lane 2) and rat (mixture of day 3 and day 5 sera) (lane 4). Interestingly, a band at ~90 kDa was detected in anti-$NRP1^B$ treated (lane 2), but not in the untreated mouse serum (lane 1). The 90 kDa circulating NRP1 might be below the detection limit in untreated mouse serum.

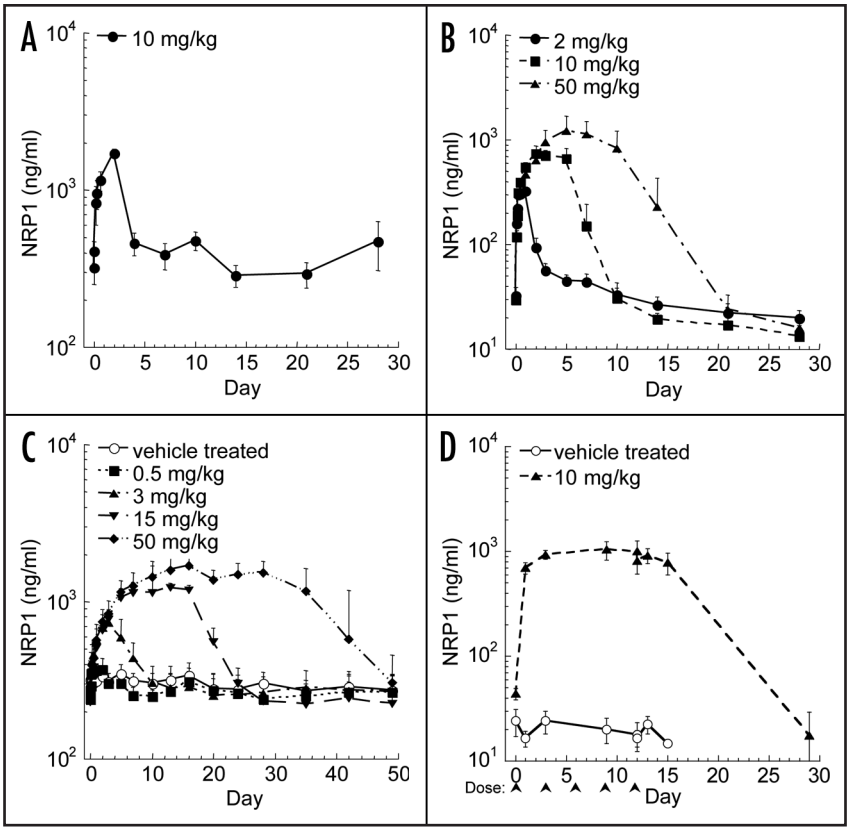

Figure 1. Circulating NRP1 concentration versus time profiles. (A) Circulating NRP1 increases in athymic nude mice receiving a single intravenous bolus dose of 10 mg/kg anti-NRP1^B. Serum samples were collected post-dose at the following time points: 15 minutes; 1, 4, 8 and 16 hours; and 2, 4, 7, 10, 14, 21 and 28 days. Error bars are standard deviations of four animals per time point. (B) Circulating NRP1 increases dose-dependently in Sprague-Dawley rats receiving a single intravenous bolus dose of 2, 10 or 50 mg/kg anti-NRP1^B. Serum samples were collected pre-dose and at the following post-dose time points: 15 minutes; 2, 4, 8, 12 and 24 hours; and 2, 3, 5, 7, 10, 14, 21 and 28 days. Concentrations of circulating NRP1 in prebleed were 21 ± 4, 20 ± 9 and 22 ± 5 ng/ml for dose groups of 2, 10 and 50 mg/kg, respectively. N = 3 animals per time point. (C) Circulating NRP1 increases dose-dependently in cynomolgus monkeys receiving a single intravenous dose of 0, 0.5, 3, 15 or 50 mg/kg anti-NRP1^B. Serum samples were collected at pre-dose and the following post-dose time points: 10 and 45 minutes; 2, 4, 7, 12 and 24 hours; and 2, 3, 5, 7, 10, 13, 16, 20, 24, 28, 35, 42, 49 and 56 days. Concentrations of circulating NRP1 in prebleed were 271 ± 13, 304 ± 118, 268 ± 125 and 258 ± 70 ng/ml for dose groups of 0.5, 3, 15 and 50 mg/kg, respectively. N = 4 animals per time point. (D) Circulating NRP1 levels in rats receiving multiple doses of 10 mg/kg anti-NRP1^B. Sprague-Dawley rats received five intravenous doses of vehicle or 10 mg/kg anti-NRP1^B on days 0, 3, 6, 9 and 12. Serum samples were collected at the following time points for both groups: day 0, 15 minutes post-dose, day 1, day 3 pre-dose, day 9 pre-dose, day 12 pre-dose and 15 minutes post-dose, day 13 and day 15; and day 29 for the anti-NRP1^B dose group. N = 3 animals per time point. Symbols represent mean ± standard deviation for (A and D) and mean + standard deviation for (B and C) for clarity.

Circulating NRP1 proteins in serum from anti-NRP1^B treated or untreated cynomolgus monkeys were analyzed by western blotting using the rabbit anti-human sNRP1 antibody. A major 90 kDa protein and a minor 120 kDa protein band were observed before treatment (Fig. 2B, lane 1). After 50 mg/kg anti-NRP1^B administration, both bands showed an increase in intensity in day 35 serum from the same animal. Thus, western blot analysis confirmed the circulating NRP1 increases in mouse, rat and monkey sera detected by ELISA.

To detect human circulating NRP1 isoforms, anti-NRP1^B (Fig. 2C, lane 2) or an isotype control (lane 1) antibody was added to normal human serum and immunoprecipitated. The rabbit anti-human sNRP1 antibody detected anti-NRP1^B associated proteins at ~120, 90 and 75 kDa (lane 2). The 90 kDa doublet and the 75 kDa bands could correspond to the sNRP1 isoforms cloned in human.[15-17] The molecular weight of the 120 kDa protein corresponds to the NRP1 ECD that contains not only the ligand binding domains, but also the MAM domain. Indeed, MAM domain peptides were detected by mass spectrometry in the 120 kDa (Fig. 3), but not the 90 kDa human NRP1 doublet band (data not shown).

Discussion

In this report, we quantified circulating NRP1 levels in mouse, rat, monkey and human sera using ELISAs. We detected putative sNRP1 proteins of ~64 kDa in mouse, 75 kDa in rat, 90 kDa in monkey, and 90 and 75 kDa in human sera by western blot. In addition to the sNRP1 proteins, we also detected a 120 kDa complete NRP1 ECD protein in human serum by mass spectrometry. The 120 kDa ECD band was also detected in mouse, rat, monkey and human sera by western blot. These results provide the first evidence, to our knowledge, that circulating NRP1 ECD may be present in serum.

After the administration of anti-NRP1^B to animals, we observed anti-NRP1^B dose-dependent increases of total circulating NRP1 (free and anti-NRP1^B bound). It has been reported that the formation of complexes between an antibody and its soluble antigen can decrease the rate of antigen clearance in vivo.[19,20] Accordingly, complexes of circulating NRP1 and anti-NRP1^B might have a longer half-life than free NRP1, thereby resulting in increased total circulating NRP1 in treated animals. Whether increased circulating NPR1 affect drug clearance needs further investigation. Although increased circulating NRP1 was observed within an hour after dosing, the possibility that anti-NRP1^B treatment accelerates sNRP1 synthesis at later time points cannot be excluded.

It has been demonstrated that antibody drug treatment can regulate the release of antigen extracellular domains by proteolytic cleavage.[21,22] We observed greater increases in the intensity of the NRP1 ECD band than the lower molecular weight sNRP1 bands in anti-NRP1^B treated animals, suggesting that anti-NRP1^B induces membrane NRP1 shedding in addition to reducing clearance of antibody-bound circulating NRP1. Recently, Swendeman, et al. reported NRP1 shedding by the metalloprotease ADAM10

in cell lines overexpressing NRP1.[23] Interestingly, another human monoclonal antibody anti-NRP1^{A}, which binds to a1a2 domain of NRP1, did not result in increased circulating NRP1. Binding of anti-NRP1^{B} to the b1b2 domain could potentially change NRP1 conformation, making it more accessible to metalloprotease cleavage.

The biological functions of sNRP1 are not yet completely understood. The recombinant human sNRP1 proteins were reported to sequester $VEGF_{165}$ and inhibit breast cancer cell migration.[15] Overexpression of the 90 kDa human sNRP1 in rat prostate carcinoma cells showed antitumor activity.[16] Mouse sNRP1 expression targeted to skin in transgenic mice inhibited vascular permeability, suggesting a role for sNRP1 in regulating vascular function.[18] Given that the 120 kDa NRP1 ECD contains the b1b2 VEGF binding domain, it may have similar biological functions as sNRP1. Whether shedding of NRP1 by anti-NRP1^{B} antibody may enhance the antibody's effect in anti-angiogenesis requires further investigation.

Materials and Methods

Rodent and primate circulating NRP1 ELISAs. To measure rodent circulating NRP1, NUNC (Neptune, NJ) 384 well Maxisorp immunoplates were coated with goat anti-rat NRP1 ECD antibody (R&D Systems, Inc., Minneapolis, MN) at 1 μg/ml. His-tagged mouse sNRP1 (641 amino acids) with an apparent molecular weight of 90 kDa (Genentech, Inc., South San Francisco) was purified from Chinese hamster ovary cells and used as a standard for both mouse and rat sera. Standards (0.0094–1.2 ng/ml) and sera diluted in PBS containing 0.5% bovine serum albumin, 0.35 M NaCl, 0.25% CHAPS, 5 mM EDTA, 0.05% Tween-20 and 15 ppm Proclin were incubated on the plates for 2 hours at room temperature. Bound analyte was detected with biotinylated goat anti-rat NRP1 ECD at 0.5 μg/ml, followed by horseradish peroxidase-conjugated streptavidin (GE Healthcare, Piscataway, NJ). The anti-rat NRP1 ECD polyclonal antibody can potentially react with all three domains (a1a2, b1b2 and c domains) of NRP1 ECD. Plates were developed using 3,3',5,5'-tetramethyl benzidine (KPL, Inc., Gaithersburg, MD). Absorbance at 450 nm was measured on a Multiskan Ascent reader (Thermo Scientific, Hudson, NH). Concentrations were determined from the standard curve using a four-parameter non-linear regression program.

Similar procedures described above were followed for primate circulating NRP1 ELISA using rabbit anti-human sNRP1 polyclonal antibody (Genentech, Inc.,) as both coat and detection. This antibody can potentially react with the a1a2 and b1b2 domains. His-tagged human sNRP1 (641 amino acids; ~85 kDa) or cynomolgus monkey sNRP1 (643 amino acids; ~95 kDa) produced at Genentech was used as the standard. Standard curve ranges for measuring human and monkey circulating NRP1 were 0.02–2.5 ng/ml and 0.03–4 ng/ml, respectively.

Western blot and mass spectrometry analysis of circulating NRP1. Circulating NRP1 isoforms in serum from untreated or anti-NRP1^{B} treated rodents and monkeys were immunoprecipitated with goat anti-rat NRP1 ECD and rabbit anti-human sNRP1 antibody-conjugated beads (CNBr Sepharose 4B, GE Healthcare, Piscataway, NJ), respectively. Human circulating NRP1 species bound to anti-NRP1^{B} mouse IgG2a were immunoprecipitated with goat anti-mouse IgG Fc (Jackson ImmunoResearch, West Grove, PA) antibody-conjugated beads. The anti-NRP1^{B} mouse IgG2a antibody contains variable domains of the anti-NRP1^{B} human IgG1 and constant domains of mouse IgG2a. Immunoprecipitated proteins were separated by 4–20% SDS-PAGE, transferred to nitrocellulose membranes (Invitrogen, Carlsbad, CA), and probed with goat anti-rat NRP1 ECD for rodent sera or rabbit anti-human sNRP1 antibody for primate sera.

Circulating NRP1 proteins in human serum were purified using an anti-NRP1^{B} coupled Sepharose affinity column. Proteins were released from the beads by boiling in sample buffer with 50 mM DTT (Pierce, Rockford, IL) and alkylated in 0.2 M

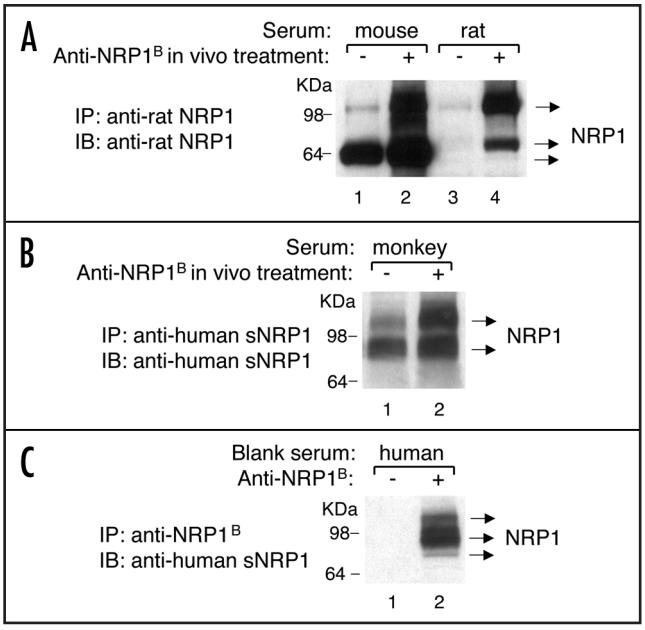

Figure 2. Western blot analysis of circulating NRP1. (A) Circulating NRP1 proteins in sera from untreated or anti-NRP1^{B} treated rodents. Serum (100 μl) from 10 mg/kg anti-NRP1^{B} human IgG1 treated mouse (day 2) (lane 2) or rat (mixture of day 3 and day 5) (lane 4) and equal volume of untreated mouse (lane 1) or rat (lane 3) serum with the addition of a matching amount (~2 μg) of anti-NRP1^{B} antibody were incubated with goat anti-rat NRP1 ECD antibody-conjugated beads. The immunoprecipitated (IP) proteins from both mouse and rat sera were separated on the same gel, and the membrane was immunoblotted (IB) with the goat anti-rat NRP1 ECD antibody. (B) Circulating NRP1 proteins in untreated and anti-NRP1^{B} treated cynomolgus monkey sera. Serum (100 μl) from 50 mg/kg anti-NRP1^{B} human IgG1 treated monkey (day 35) (lane 2) and an equal volume of serum from the same monkey before treatment (lane 1) with the addition of a matching amount (~5 μg) of anti-NRP1^{B} antibody were incubated with rabbit anti-human sNRP1 antibody-conjugated beads. The immunoprecipitated proteins were immunoblotted with the rabbit anti-human sNRP1 antibody. These results are representative of sera from four individual animals. (C) Circulating NRP1 proteins in pooled sera from untreated humans. The amount of 2 μg anti-NRP1^{B} mouse IgG2a (lane 2) or isotype control antibody (lane 1) was added to 200 μl blank human serum pool. The antibodies were immunoprecipitated with goat anti-mouse IgG Fc antibody-conjugated beads, and the associated proteins were immunoblotted with rabbit anti-human sNRP1 antibody.

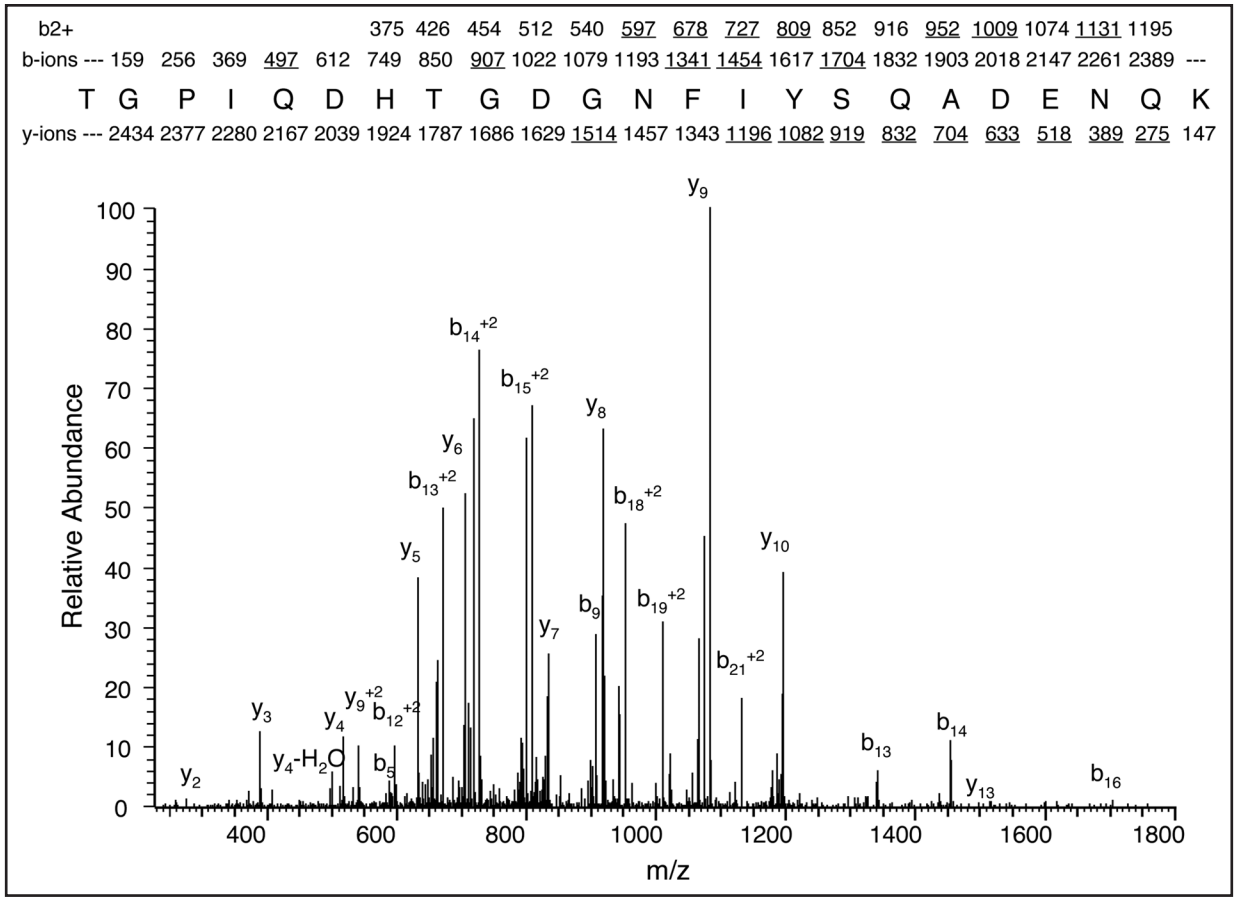

Figure 3. Tandem mass spectrometry analysis confirms the presence of the MAM domain in the 120 kDa circulating NRP1 protein. Affinity purified circulating NRP1 proteins from human serum were separated by SDS-PAGE. The 120 kDa gel band was digested with trypsin and analyzed. The most abundant protein hit was human NRP1. Total protein coverage was 31% and three peptides from the MAM domain (amino acids 650–811) were identified. The representative peptide shown above covers residues 680–702 (mass/charge = 845.71, charge = 3) where matched peaks are underlined. *b*-ions originating from the N-terminus and *y*-ions originating from the C-terminus of the peptide are labeled as per the standard nomenclature convention of Andersson and Porath.[24]

iodoacetamide (Sigma, St. Louis, MO). Samples were separated by 4–20% SDS-PAGE and stained with Coomassie Brilliant Blue. Gel bands were excised, washed in 25 mM ammonium bicarbonate (Sigma) containing 5% acetonitrile (Burdick and Jackson, Muskegon, MI) for 20 min followed by 25 mM ammonium bicarbonate in 50:50 acetonitrile:water for another 20 min. Gel pieces were dehydrated in acetonitrile and digested with 0.2 µg trypsin (Promega, Madison, WI) in 25 mM ammonium bicarbonate, pH 8, overnight at 37°C.

Peptides were extracted from the gel slices in 15 µl of 10% acetic acid (J.T. Baker, Phillipsburg, NJ), followed by 50 µl of 0.1% trifluoroacetic acid (Applied Biosystems, Foster City, CA) containing 5% acetonitrile, and finally with 50 µl of pure acetonitrile. Extractions were pooled and reduced in volume to 8 µl. Samples were injected onto a C18 column at a flow rate of 1 µl/min using a Waters nano-Acquity Ultra Pressure Liquid Chromatography under gradient conditions. Samples were analyzed on-line via nanospray ionization into an Orbitrap mass spectrometer (Thermo, San Jose, CA). Data was collected in data dependent mode with the parent ion being analyzed in the Orbitrap and the top ten most abundant ions being selected for fragmentation and analysis in the ion trap. Tandem mass spectrometric data were analyzed using the search algorithm Mascot (Matrix Sciences, London, UK) with an ion cutoff score of 20.

Acknowledgements

We thank Helen Bai and Herman Wong for running circulating NRP1 ELISAs, Kwame Hoyte for helping purify NRP1 from human serum, Laura DeForge and Katherine Kozak for helpful discussions and Anne Wong for editing.

References

1. He Z, Tessier-Lavigne M. Neuropilin is a receptor for the axonal chemorepellent Semaphorin III. Cell 1997; 90:739-51.
2. Kolodkin AL, Levengood DV, Rowe EG, Tai YT, Giger RJ, Ginty DD. Neuropilin is a semaphorin III receptor. Cell 1997; 90:753-62.
3. Soker S, Takashima S, Miao HQ, Neufeld G, Klagsbrun M. Neuropilin-1 is expressed by endothelial and tumor cells as an isoform-specific receptor for vascular endothelial growth factor. Cell 1998; 92:735-45.
4. Kitsukawa T, Shimono A, Kawakami A, Kondoh H, Fujisawa H. Overexpression of a membrane protein, neuropilin, in chimeric mice causes anomalies in the cardiovascular system, nervous system and limbs. Development 1995; 121:4309-18.
5. Kawasaki T, Kitsukawa T, Bekku Y, Matsuda Y, Sanbo M, Yagi T, et al. A requirement for neuropilin-1 in embryonic vessel formation. Development 1999; 126:4895-902.
6. Kitsukawa T, Shimizu M, Sanbo M, Hirata T, Taniguchi M, Bekku Y, et al. Neuropilin-semaphorin III/D-mediated chemorepulsive signals play a crucial role in peripheral nerve projection in mice. Neuron 1997; 19:995-1005.

7. Kawakami A, Kitsukawa T, Takagi S, Fujisawa H. Developmentally regulated expression of a cell surface protein, neuropilin, in the mouse nervous system. J Neurobiol 1996; 29:1-17.
8. Nakamura F, Goshima Y. Structural and functional relation of neuropilins. Adv Exp Med Biol 2002; 515:55-69.
9. Cai H, Reed RR. Cloning and characterization of neuropilin-1-interacting protein: a PSD-95/Dlg/ZO-1 domain-containing protein that interacts with the cytoplasmic domain of neuropilin-1. J Neurosci 1999; 19:6519-27.
10. Chen H, He Z, Bagri A, Tessier-Lavigne M. Semaphorin-neuropilin interactions underlying sympathetic axon responses to class III semaphorins. Neuron 1998; 21:1283-90.
11. Fujisawa H. From the discovery of neuropilin to the determination of its adhesion sites. Adv Exp Med Biol 2002; 515:1-12.
12. Mamluk R, Gechtman Z, Kutcher ME, Gasiunas N, Gallagher J, Klagsbrun M. Neuropilin-1 binds vascular endothelial growth factor 165, placenta growth factor-2, and heparin via its b1b2 domain. J Biol Chem 2002; 277:24818-25.
13. Liang WC, Dennis MS, Stawicki S, Chanthery Y, Pan Q, Chen Y, et al. Function blocking antibodies to neuropilin-1 generated from a designed human synthetic antibody phage library. J Mol Biol 2007; 366:815-29.
14. Pan Q, Chanthery Y, Liang WC, Stawicki S, Mak J, Rathore N, et al. Blocking neuropilin-1 function has an additive effect with anti-VEGF to inhibit tumor growth. Cancer Cell 2007; 11:53-67.
15. Cackowski FC, Xu L, Hu B, Cheng SY. Identification of two novel alternatively spliced Neuropilin-1 isoforms. Genomics 2004; 84:82-94.
16. Gagnon ML, Bielenberg DR, Gechtman Z, Miao HQ, Takashima S, Soker S, et al. Identification of a natural soluble neuropilin-1 that binds vascular endothelial growth factor: In vivo expression and antitumor activity. Proc Natl Acad Sci USA 2000; 97:2573-8.
17. Rossignol M, Gagnon ML, Klagsbrun M. Genomic organization of human neuropilin-1 and neuropilin-2 genes: identification and distribution of splice variants and soluble isoforms. Genomics 2000; 70:211-22.
18. Mamluk R, Klagsbrun M, Detmar M, Bielenberg DR. Soluble neuropilin targeted to the skin inhibits vascular permeability. Angiogenesis 2005; 8:217-27.
19. Hsei V, Deguzman GG, Nixon A, Gaudreault J. Complexation of VEGF with bevaczumab decreases VEGF clearance in rats. Pharm Res 2002; 19:1753-6.
20. Casale TB, Bernstein IL, Busse WW, LaForce CF, Tinkelman DG, Stoltz RR, et al. Use of an anti-IgE humanized monoclonal antibody in ragweed-induced allergic rhinitis. J Allergy Clin Immunol 1997; 100:110-21.
21. Petrelli A, Circosta P, Granziero L, Mazzone M, Pisacane A, Fenoglio S, et al. Ab-induced ectodomain shedding mediates hepatocyte growth factor receptor downregulation and hampers biological activity. Proc Natl Acad Sci USA 2006; 103:5090-5.
22. Molina MA, Codony-Servat J, Albanell J, Rojo F, Arribas J, Baselga J. Trastuzumab (herceptin), a humanized anti-Her2 receptor monoclonal antibody, inhibits basal and activated Her2 ectodomain cleavage in breast cancer cells. Cancer Res 2001; 61:4744-9.
23. Swendeman S, Mendelson K, Weskamp G, Horiuchi K, Deutsch U, Scherle P, et al. VEGF-A stimulates ADAM17-dependent shedding of VEGFR2 and crosstalk between VEGFR2 and ERK signaling. Circ Res 2008; 103:916-8.
24. Andersson L, Porath J. Isolation of phosphoproteins by immobilized metal (Fe^{3+}) affinity chromatography. Anal Biochem 1986; 154:250-4.